Supporting Information

Theoretical formulation of $Li_{3a+b}N_aX_b$ (X= Halogen) as potential artificial solid electrolyte interphases (ASEI) to protect Li anode

*Junwu Sang, Yuran Yu, Zhuo Wang * and Guosheng Shao **

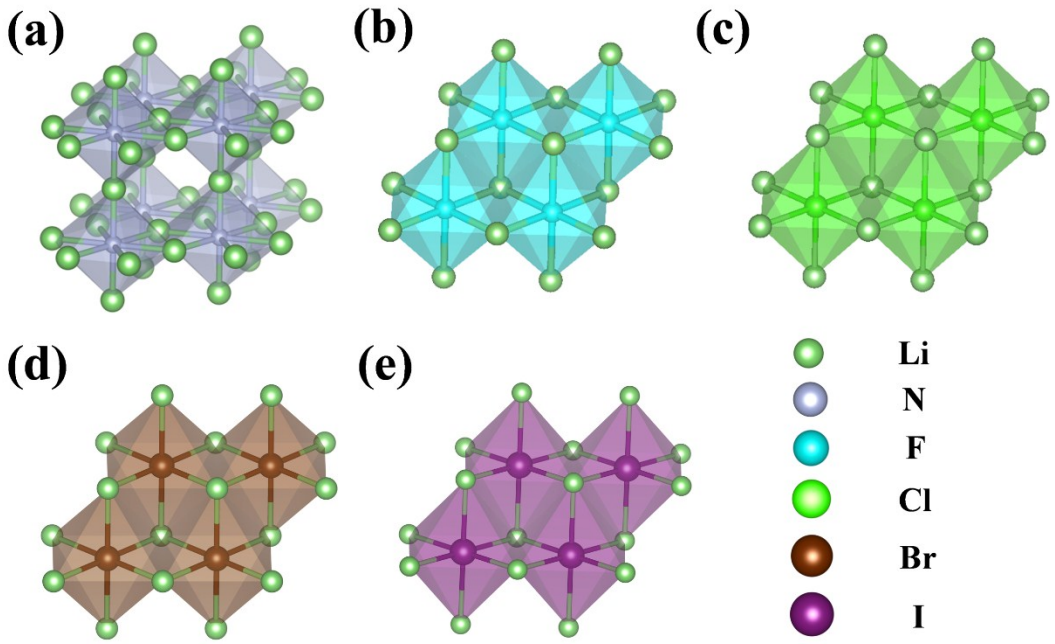

Fig. S1 Structural configurations of (a) Li_3N, (b) LiX (X = F, Cl, Br, I).

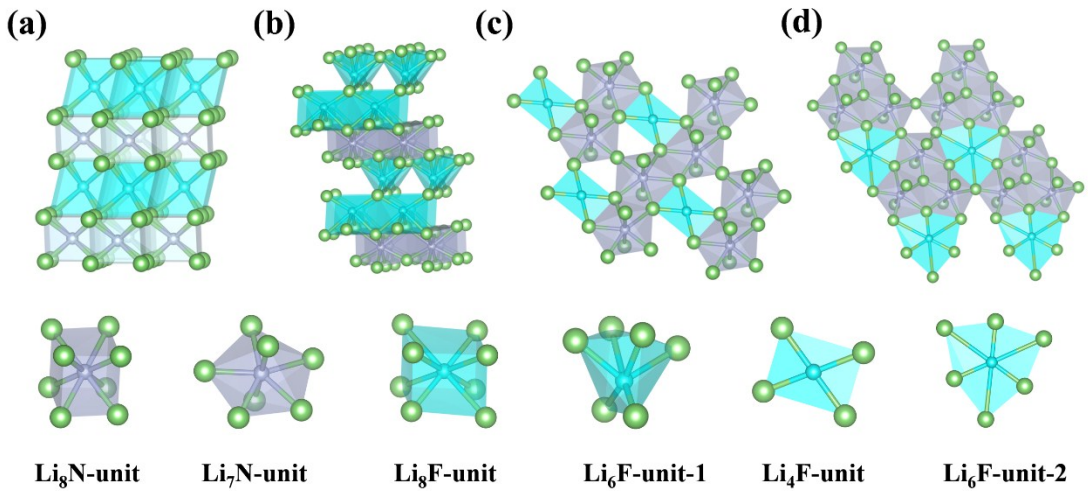

Fig. S2 Structures from USPEX energy minimization for (a) Li_4NF, (b) Li_5N_2F, (c) Li_7N_2F, and (d) $Li_{10}N_3F$.

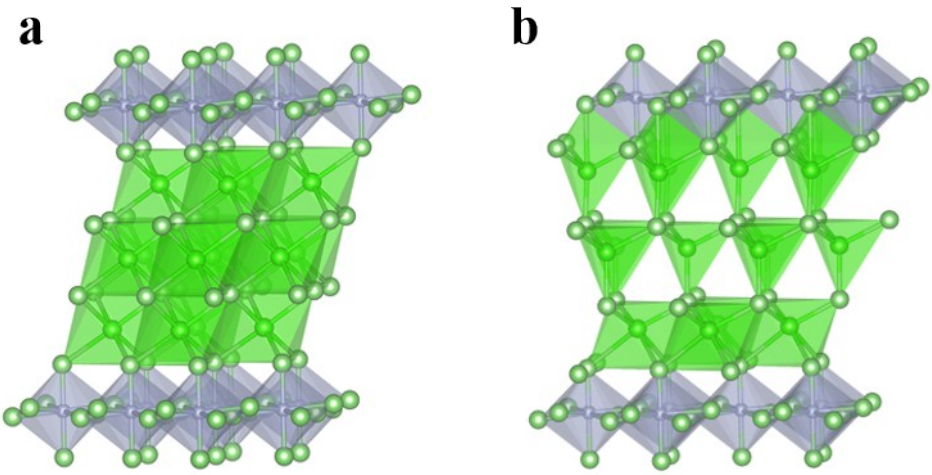

Fig. S3 Structural configuration of (a) Li_6NCl_3 predicted by USPEX with the symmetry of $P\bar{3}m1$ (164), (b) Li_6NCl_3 from Materials Project webpage with the symmetry of Cm (8).

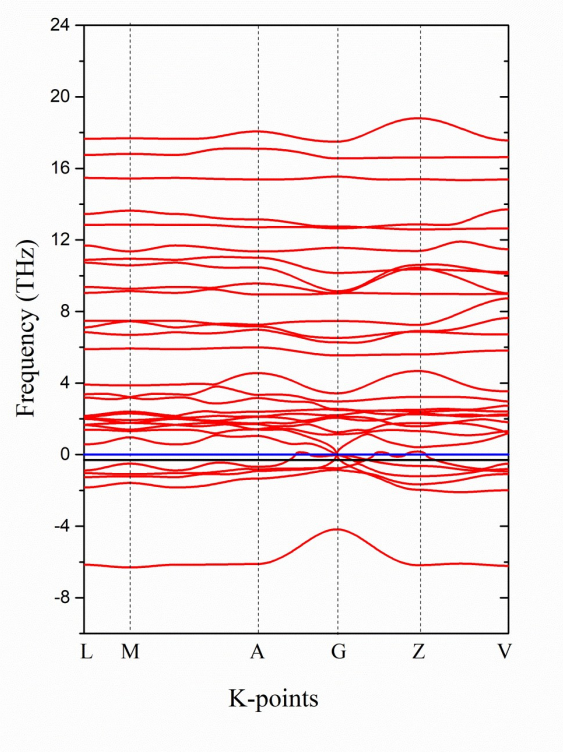

Fig. S4 Phonon band structure of Li_6NI_3. (blue line: 0 THz, black line: -0.3 THz)

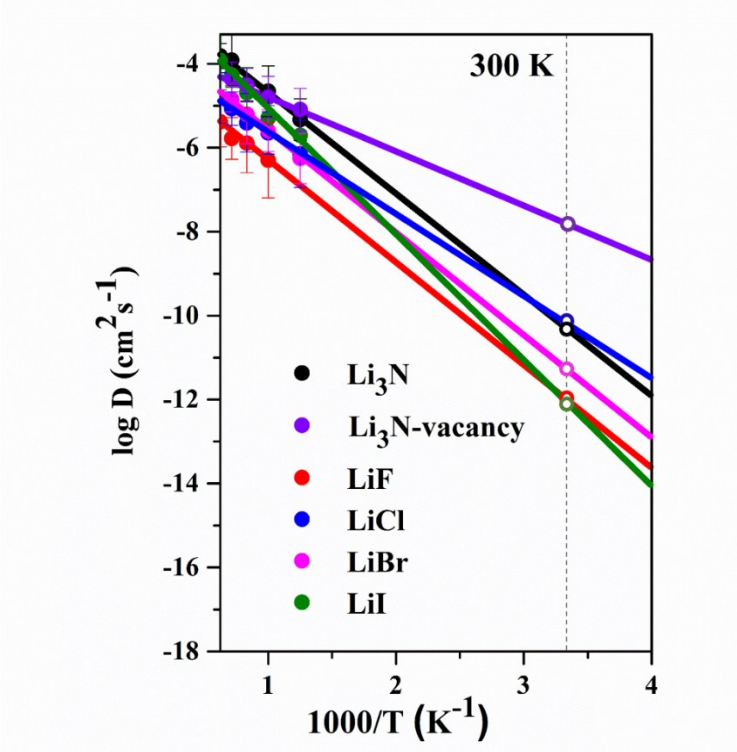

Fig. S5 Diffusion coefficients for lithium ions from AIMD simulation. The extrapolated D values at room temperature are presented by open patterns on the right.

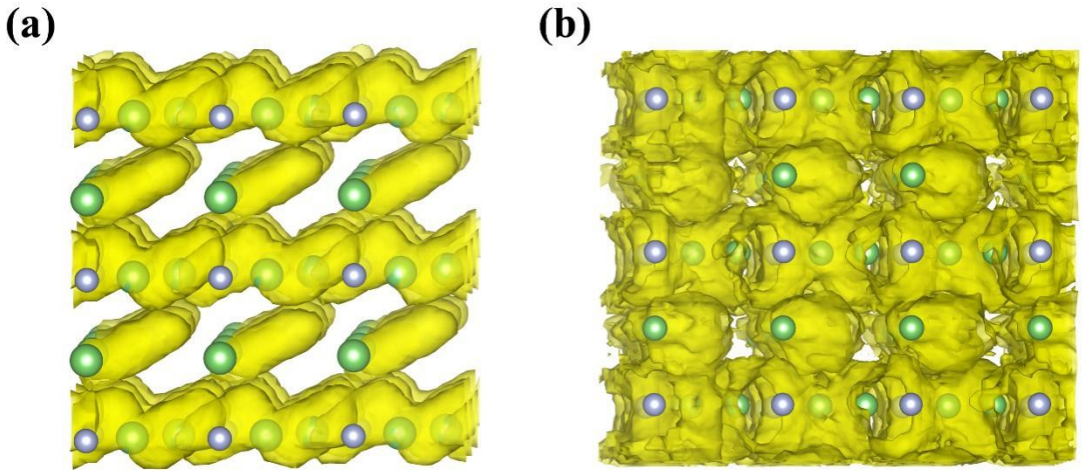

Fig. S6 Diffusion trajectories of Li^+ ions after 180 ps at 1000 K for (a) Li_3N and (b) Li_3N-vacancy. The yellow regions show the lithium ion diffusion path, with the Isosurface level being 2×10^{-6}.

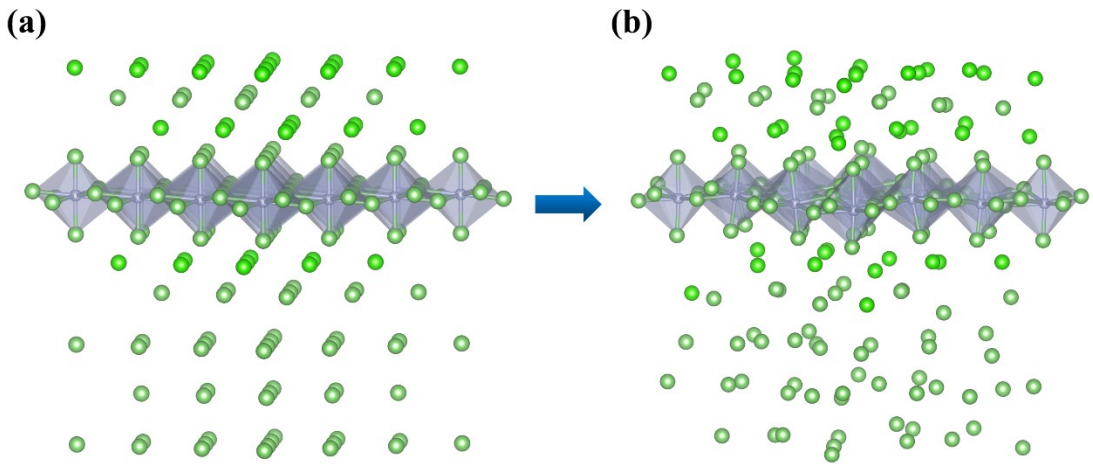

Fig. S7 Interfaced Li_6NCl_3|Li (a) before, (b) after AIMD simulations at 500 K for 200 ps.

Physical Chemistry Chemical Physics

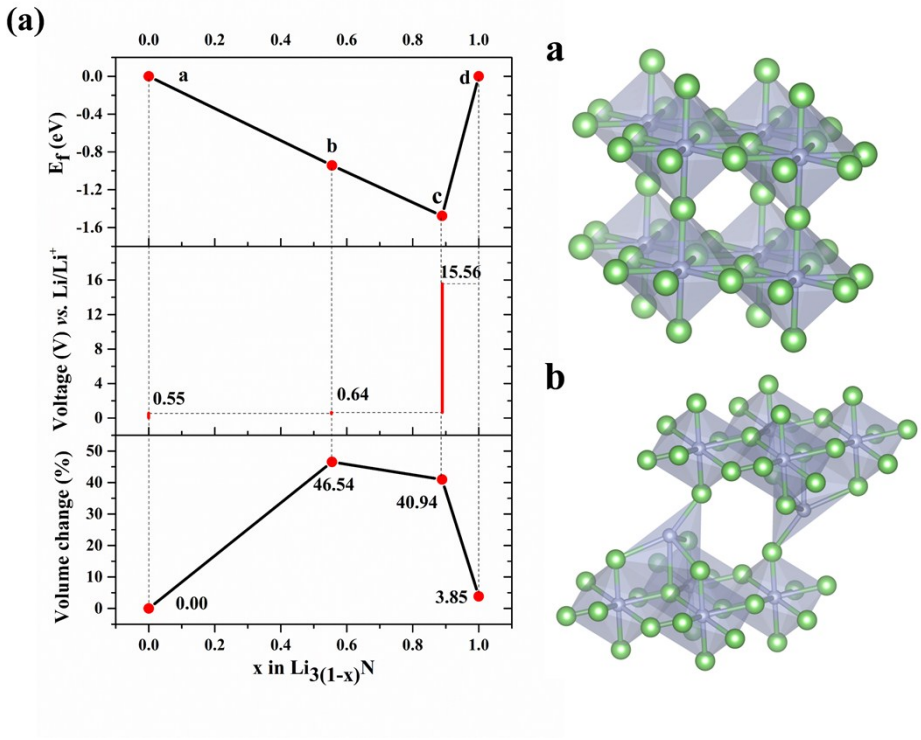

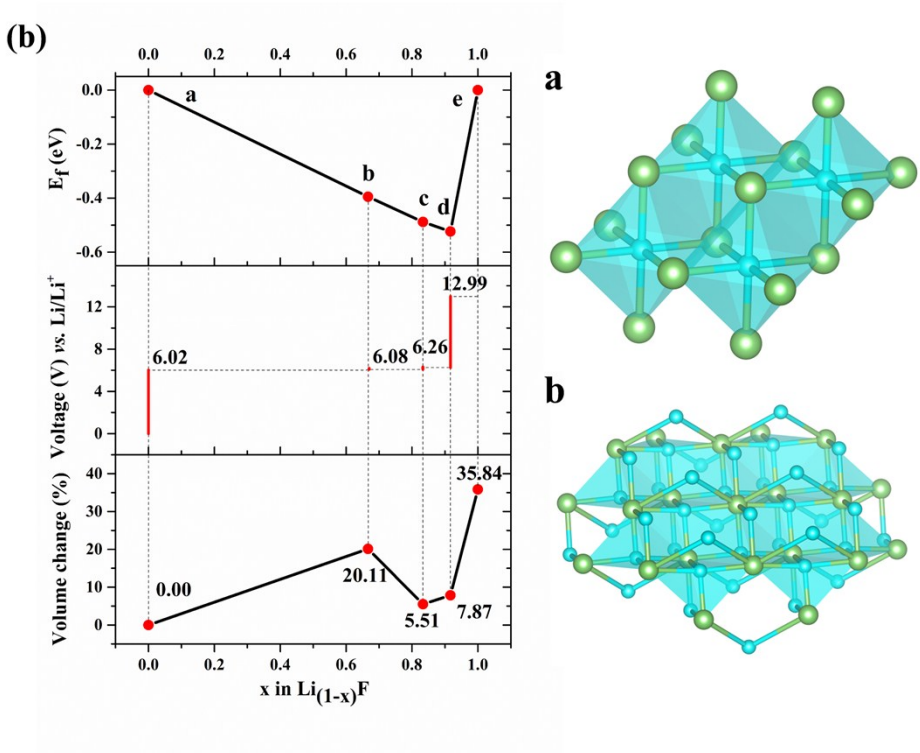

Physical Chemistry Chemical Physics

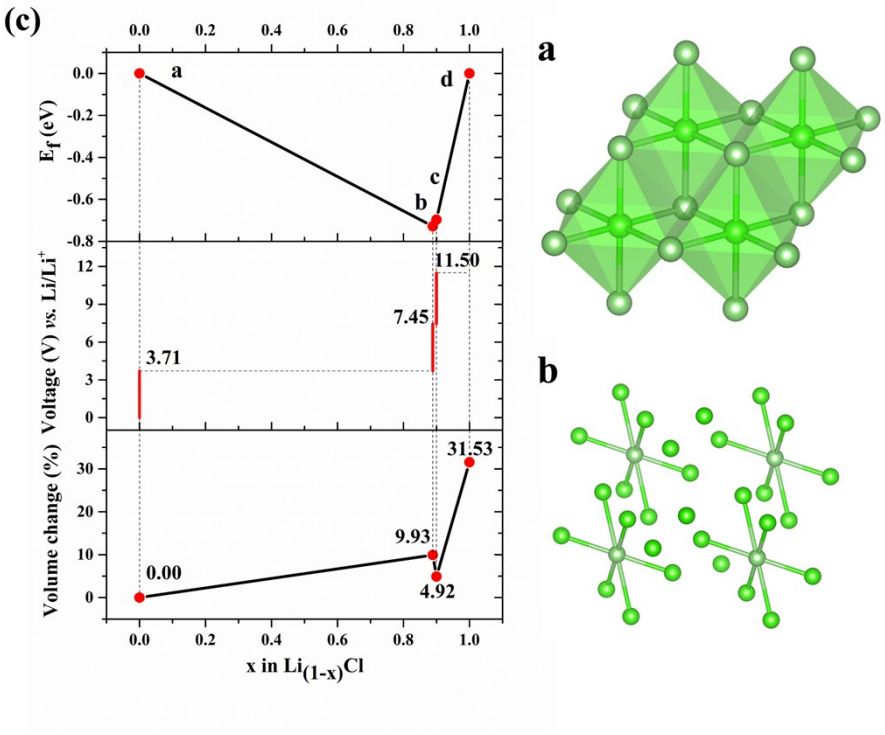

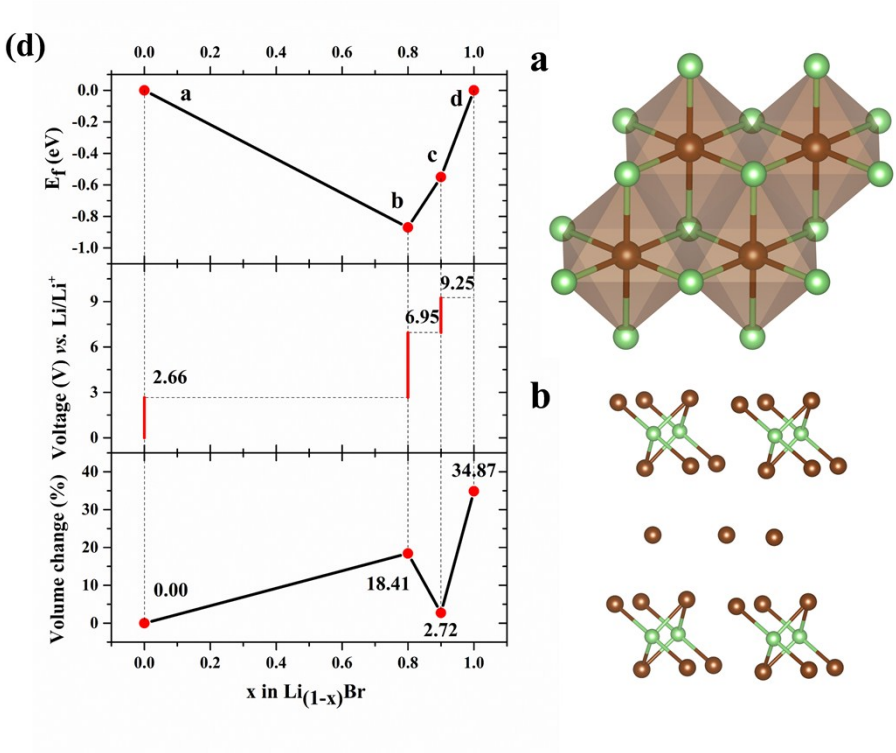

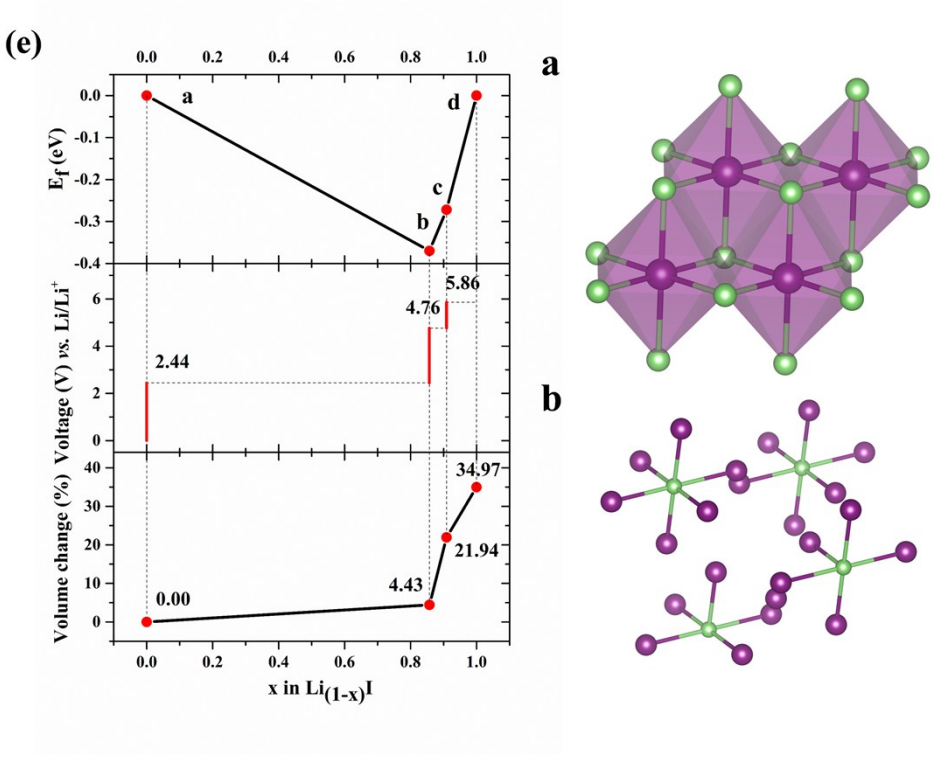

Fig. S8 The energy convex hulls, voltage plateau, and volume change rate during the process of Li^+ depletion through ATAT simulation for (a) $Li_{3(1-x)}N$ ($0 \leq x \leq 1$) (b) $Li_{(1-x)}F$ ($0 \leq x \leq 1$) (c) $Li_{(1-x)}Cl$ ($0 \leq x \leq 1$) (d) $Li_{(1-x)}Br$ ($0 \leq x \leq 1$) (e) $Li_{(1-x)}I$ ($0 \leq x \leq 1$). The structures for some stable interphases are displayed on the right side.

Physical Chemistry Chemical Physics

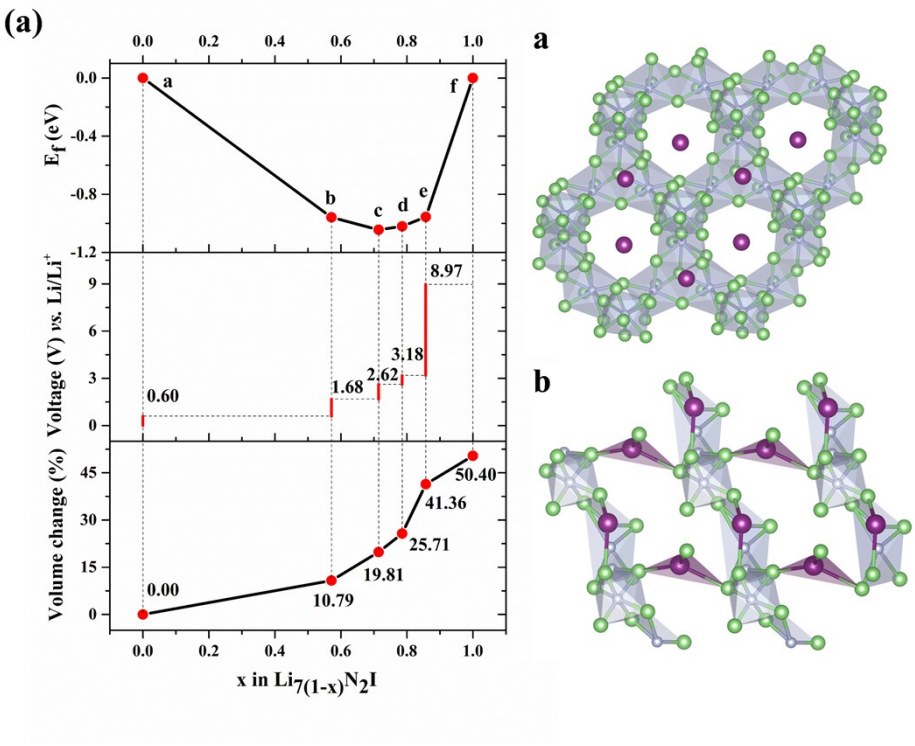

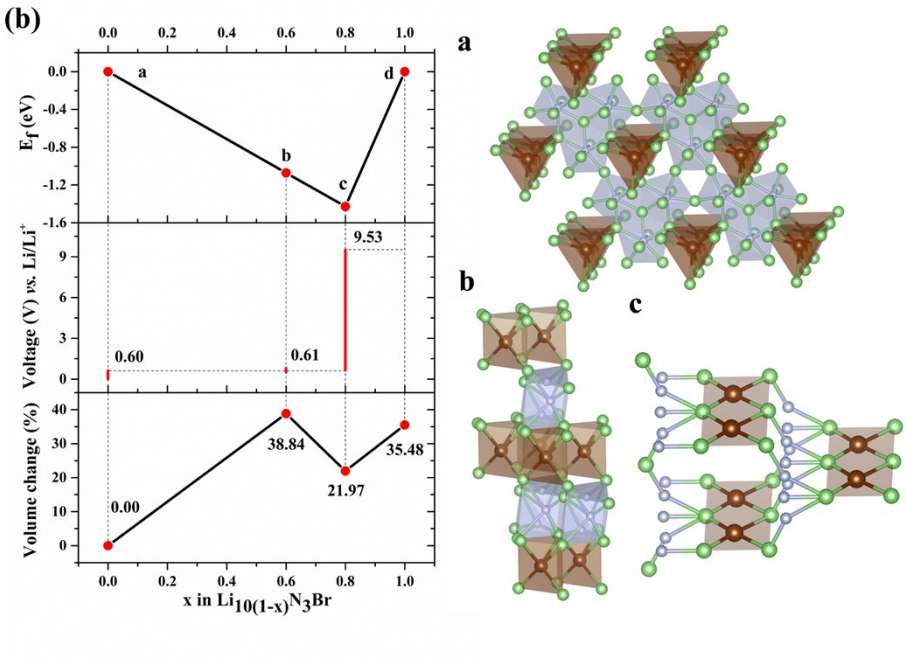

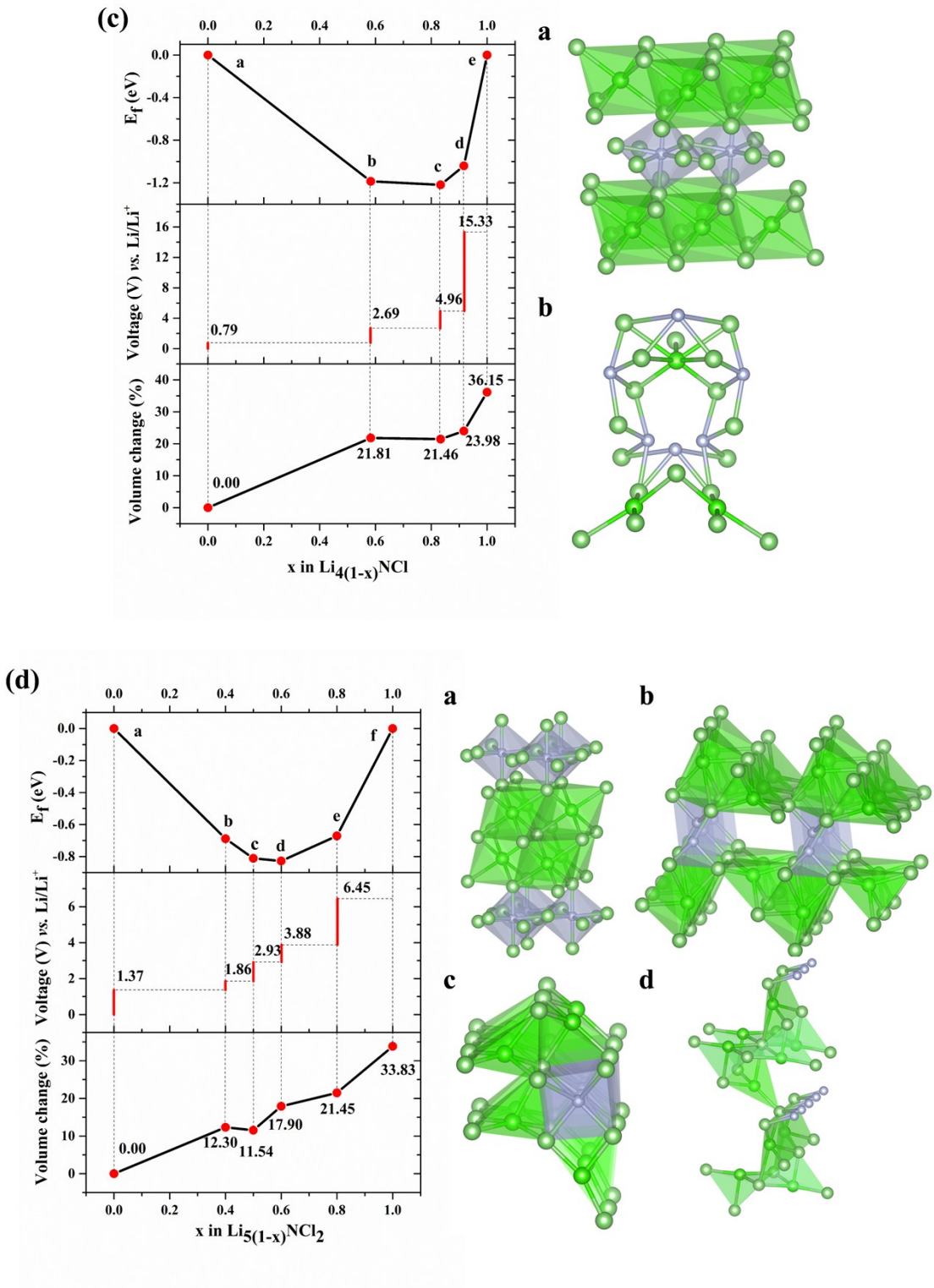

Fig. S9 The convex hulls, voltage plateau, and volume change rate during the process of Li^+ depletion through ATAT simulation for (a) $Li_{7(1-x)}N_2I$ ($0 \leq x \leq 1$) (b) $Li_{10(1-x)}N_3Br$ ($0 \leq x \leq 1$) (c) $Li_{4(1-x)}NCl$ ($0 \leq x \leq 1$), and (d) $Li_{5(1-x)}NCl_2$ ($0 \leq x \leq 1$). The structures for some stable interphases are displayed on the right side.

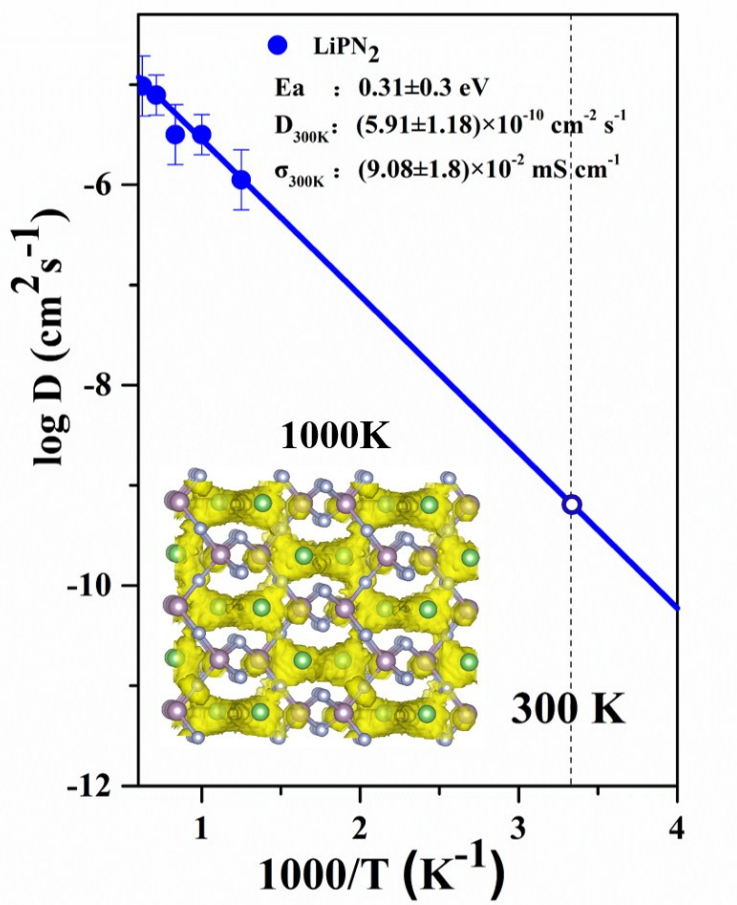

Fig. S10 Diffusion coefficients (D) for lithium ions in $LiPN_2$ from AIMD simulation. Some useful information, including of E_a activation barrier, Diffusion coefficients D_{300K} at 300 K, Li^+ ionic conductivity σ_{300K} at 300 K, and diffusion trajectories of Li^+ ions at 1000 K, are in insets.

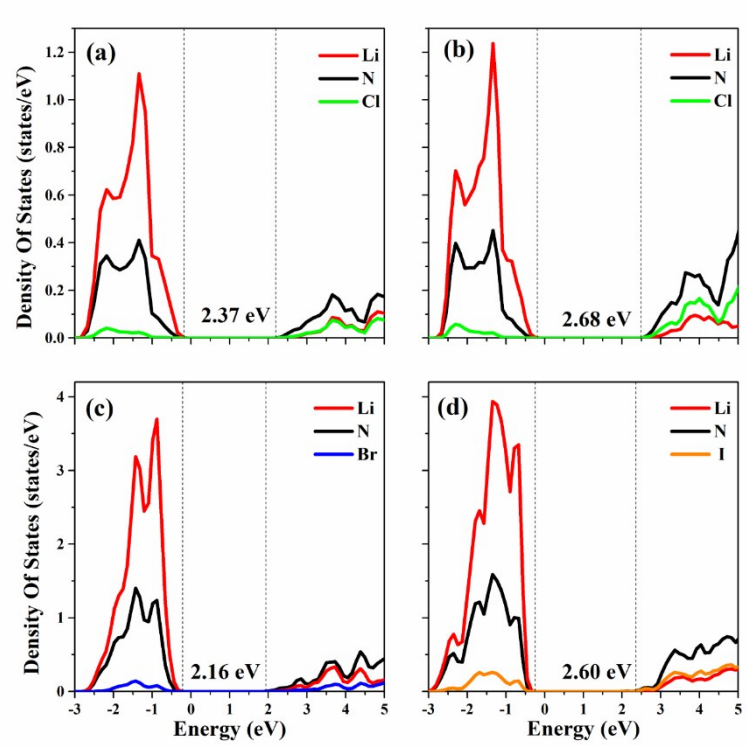

Fig. S11 The projected density of states calculated using the HSE06 functional for (a) Li_4NCl, (b) Li_6NCl_3, (c) $Li_{10}N_3Br$, (d) Li_7N_2I.

Table S1 Summary of data for the Li^+ ionic conductivities of referential compounds.

System	E_a (eV)	D_{300K} (cm^{-2} s^{-1})	σ_{300K} (mS cm^{-1})
Li_3N	0.48±0.07	(4.83±1.35) $\times10^{-11}$	(2.04±0.57) $\times10^{-2}$
Li_3N-vacancy	0.28±0.03	(1.23±0.14) $\times10^{-8}$	5.07±0.56
LiF	0.45±0.08	(2.73±0.82) $\times10^{-12}$	(9.84±2.95) $\times10^{-4}$
LiCl	0.42±0.06	(3.14±0.81) $\times10^{-11}$	(5.56±0.15) $\times10^{-3}$
LiBr	0.52±0.08	(2.2±0.64×) 10^{-12}	(6.45±×1.87) $\times10^{-4}$
LiI	0.58±0.11	(1.32±0.44) $\times10^{-12}$	(2.96±0.98) $\times10^{-4}$
$Li_{3.92}NCl$	0.30±0.03	(8.17±0.71) $\times10^{-9}$	2.12±0.40
$Li_{4.92}NCl_2$	0.32±0.02	(3.31±0.51) $\times10^{-9}$	1.01±0.19
$Li_{5.93}NCl_3$	0.44±0.04	(5.72±0.62) $\times10^{-11}$	(1.53±0.29) $\times10^{-2}$